OMEGA NAUGHT – Paper IX

Exact Recovery on the 600-Cell

Quantization, Residue Witnesses, and Finite Histories

Matthew Alan Newman

ORCID: 0009-0007-5468-3125

5 November 2026

Draft 0.6, illustrated, for author review

Author-supplied DOI (reservation not independently verified):

10.5281/zenodo.23688676

Abstract

We study exact recovery for a quantized linear network on the 120 vertices of the regular 600-cell. Let A be its specified adjacency matrix, $M = 13I + A$, and $T(d) = \left\lfloor 339949771344778\, Md/(25 \cdot 10^{15}) \right\rfloor$ for $d \in \mathbb{Z}^{120}$. Although T is not injective, we prove that the reduced output together with the 120 predecessor residues modulo eight determines every integer input uniquely. The witness occupies exactly 360 bits, or 45 packed bytes. The proof combines an exact positive-definiteness certificate for $M - 9I$ with integer separation and the strict difference bound for equal quantization cells. An exact inverse bounds each coordinate to an interval of width less than twelve; fixing its residue leaves at most two candidates, giving a complete finite decoder. Backward induction extends recovery to every finite trajectory when its terminal state and ordered witnesses are retained. We specify coordinate order, byte packing, portable integer interchange, and history framing, and provide reproducible exact checks. The 360-bit minimum for independently representing the complete residue vector is distinguished from the minimum of an arbitrary recovery witness conditioned on the output. A separate lattice-coset and geometric argument gives $307 \le \ell^* \le 352$ for that latter problem. Its exact optimum, efficient general decoding, and application advantages remain open.

Keywords. Reversible quantization; exact recovery; 600-cell; integer separation; side information; lattice fibers; finite histories.

1 Introduction

A reduced description can identify several different original states. To reproduce the original exactly, a retained record must distinguish the states that the reduction identifies. This observation becomes a precise coding problem once the state space, reduction, and decoder information are specified. A record sufficient for one reduction need not be sufficient for another, and exact reconstruction is a different objective from producing an output that is merely similar.

This paper gives an explicit construction for one such problem. The state is an integer value at each of 120 fixed graph vertices. A positive linear averaging operator is followed by componentwise flooring. The visible output is therefore a coarser description of the predecessor. We retain three bits per coordinate: its residue modulo eight. The resulting pair is injective on the entire integer lattice:

$$d \longmapsto \big(T(d), r(d)\big), \qquad r(d) = (d_i \bmod 8)_{i=0}^{119}, \tag{1}$$

Throughout this paper, $a \bmod b := a - b\lfloor a/b \rfloor \in \{0, 1, \ldots, b-1\}$ denotes the canonical least nonnegative residue for every $a \in \mathbb{Z}$ and integer $b \geq 1$. The mathematical contribution is the specified network and the proof that this simple record is sufficient. The proof uses all coordinates jointly. It first establishes a lower bound on the image of every nonzero integer difference, then shows that equal outputs and equal residues would violate that bound. The residue encoder itself is coordinatewise and requires no enumeration of an output fiber. Decoding is provided by exact interval propagation and finite search.

Retaining information discarded by finite-precision dynamics has substantial precedent. Reversible learning algorithms retain auxiliary information to reverse training dynamics [3]; integer-to-integer transforms provide reversible representations compatible with rounding [4]. Quantization with decoder side information and lattice binning supply further relevant settings [5, 6, 7]. Our theorem concerns a deterministic, worst-case, exact-recovery guarantee for the particular operator below. It does not assert that the general principle of retained side information is new.

Two different size questions will be kept separate. Independently storing the complete residue vector requires 360 bits, and our packing attains that size. An arbitrary witness allowed to exploit the reduced output can be smaller: the separate research interval is $307 \leq \ell^* \leq 352$. The explicit 360-bit construction supplies a direct encoder and an exact finite decoder; the smaller sufficient capacity does not by itself supply a useful ranker.

1.1 Scope and information contract

The decoder knows the graph and coordinate order, rational constants, mathematical floor convention, and record format. Witness counts exclude the reduced output and any separately transmitted rules or framing. The domain is $\mathbb{Z}^{120}$, including negative and arbitrarily large coordinates. No probability distribution on the inputs is assumed. Finite witnessed histories use only the transitions specified by T.

The proof concerns mathematical states and exact finite records of those states. It does not recover unrecorded analog information. Code executions check finite premises and implementation behavior; the universal statement is the theorem proved from those premises.

2 The fixed network and exact arithmetic

2.1 Geometry, adjacency, and ordering

Let $\phi = (1 + \sqrt{5})/2$. We use the standard 120-vertex coordinate realization of the 600-cell [1]:

1. the eight permutations of $(\pm 1, 0, 0, 0)$;
2. the sixteen vectors $(\pm 1, \pm 1, \pm 1, \pm 1)/2$;
3. the ninety-six even coordinate permutations of $(0, \pm 1, \pm\phi, \pm(\phi - 1))/2$.

The three nonzero signs in the last family vary independently.

For exact implementation, a coordinate is represented by an integer pair (a, b) meaning $(a + b\phi)/2$. Vertices are sorted lexicographically as tuples of four integer pairs; this is an ordering of representations, not an instruction to round and sort real coordinates. Two vertices are adjacent when their squared Euclidean distance is $2 - \phi$. Identify a pair numerator (a, b) with $a + b\phi \in \mathbb{Z}[\phi]$. If $\eta_k = (a_k - a'_k) + (b_k - b'_k)\phi$ is the numerator difference in coordinate k, the actual coordinate difference is $\eta_k/2$. Thus adjacency is equivalent to $\sum_{k=1}^{4} \eta_k^2 = 4(2 - \phi) = 8 - 4\phi$, whose integer-pair representation is $(8, -4)$. The identity

$$(u + v\phi)^2 = (u^2 + v^2) + (2uv + v^2)\phi \tag{2}$$

makes that test entirely integral.

Let A be the adjacency matrix in this fixed order and put

$$M = 13I + A, \qquad P = M/25. \tag{3}$$

The graph is undirected and 12-regular, so M is symmetric, nonnegative, and has row and column sums 25. The geometry has four position coordinates; the mathematical state has 120 scalar coordinates attached to those vertices.

The exact fixture serialization and its digest are given in Appendix B. The digest pins the chosen bytes and labels; the coordinate construction and matrix checks supply their mathematical role. Figure 1 shows the closed neighborhood used in the capacity cover. The projected vertex geometry does not change the 120-coordinate state space.

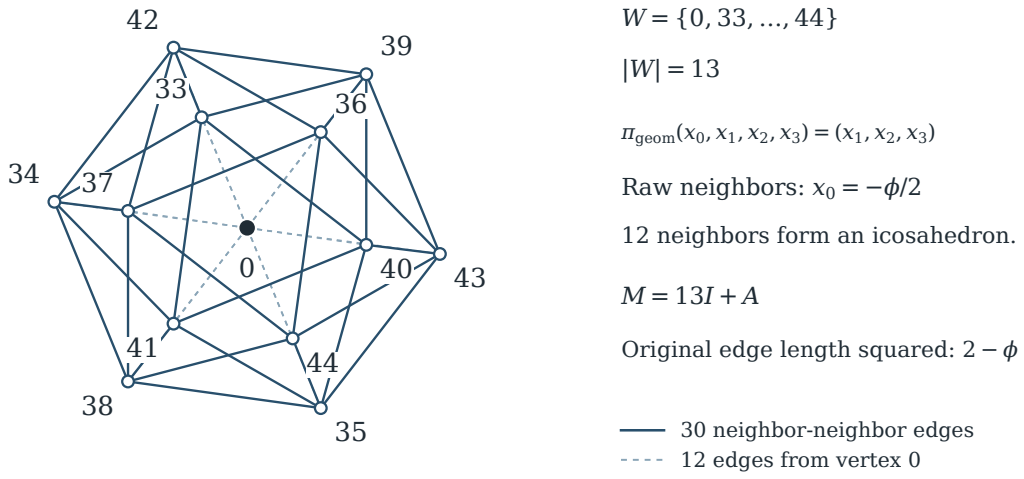


Figure 1: The closed neighborhood $W = \{0, 33, \ldots, 44\}$. Its twelve neighbors form an icosahedral graph with 30 edges; dashed segments denote the twelve edges incident to vertex zero. Labels and adjacencies are computed from the pinned fixture. The drawing applies $\pi_{\text{geom}}(x_0, x_1, x_2, x_3) = (x_1, x_2, x_3)$, followed by an orthographic view. The raw neighbors lie in $x_0 = -\phi/2$, while vertex zero is $(-1, 0, 0, 0)$. Projected segment lengths need not equal the original four-dimensional lengths. Image created by ChatGPT.

2.2 Rational quantization

Set

$$\begin{aligned} Q &= 339949771344778, \quad S = 10^{15}, \qquad\qquad D = 25S, \\ q &= Q/S, \qquad\qquad\qquad C = qP = QM/D, \quad T(d) = \lfloor Cd \rfloor . \end{aligned} \tag{4}$$

Floors are componentwise mathematical floors. In particular, flooring a negative noninteger is not truncation toward zero. The integer Q and denominator D define the operator exactly.

The OMEGA scalar reference motivates a factor $\lambda = \phi/(\phi + \pi)$. The chosen rational q is a finite implementation parameter, not an assertion that a finite decimal equals λ exactly. Replacing q by the ideal real factor defines a different flooring map on an unbounded integer domain and requires its own statement.

Before quantization, C has the familiar averaging properties

$$C\mathbf{1} = q\mathbf{1}, \qquad \overline{Cv} = q\overline{v}, \qquad \|C(v-w)\|_\infty \le q\,\|v-w\|_\infty . \tag{5}$$

Here $\mathbf{1} = (1, \dots, 1)^T \in \mathbb{Z}^{120}$ is the all-ones vector, $\overline{v} = \frac{1}{120}\sum_{i=0}^{119} v_i$ denotes the arithmetic mean of $v \in \mathbb{R}^{120}$, and $0 < q < 1$. These are statements about the real linear operator. Flooring introduces ambiguity; it does not preserve every real identity in (5).

3 Exact matrix certificates and integer separation

The following facts are checked with exact integer arithmetic. A complete standalone checker is printed in Appendix B.

Proposition 3.1 (Finite matrix certificates)**.** *For the matrix in* (3)*, $M - 9I$ is positive definite. There is an explicit integer matrix N such that*

$$MN = hI, \qquad h = 4948372000, \qquad \max_i \sum_j |N_{ij}| = 801320608. \tag{6}$$

Moreover,

$$\Delta := \det M = 2^{80}5^{27}11^{36}13^{25}41^{9}211^{4} > 0. \tag{7}$$

Certificate verification. Reconstruct the graph by (2). Fraction-free Bareiss elimination [2] gives 120 positive leading principal determinants of $M - 9I$, with every division verified to have zero remainder. Sylvester's criterion establishes positive definiteness. Separate elimination on M gives (7).

An additional exact certificate verifies $f(M) = 0$, where

$$\begin{aligned} f(x) = (x-10)(x-11)(x-13)(x-16)(x-25) \\ \cdot (x^2 - 32x + 211)(x^2 - 30x + 205). \end{aligned} \tag{8}$$

Let $g(x) = (f(x) - f(0))/x$. Then $f(0) = -5h$ and $Mg(M) = 5hI$. Evaluating $g(M)$ by exact Horner steps shows that every entry is divisible by five. Define $N = g(M)/5$; direct multiplication verifies (6), including its row norm. These operations are finite identities on explicitly constructed integer matrices. □

For comparison, the roots of (8) are $10, 11, 13, 16, 25, 16 \pm 3\sqrt{5}, 15 \pm 2\sqrt{5}$, all greater than $37/4$. Since M is symmetric, the annihilating identity also implies $\lambda_{\min}(M) > 37/4 > 9$. The leading-minor certificate verifies the weaker property needed below without numerical eigenvalue estimates.

Lemma 3.2 (Integer separation)**.** *For every nonzero $z \in \mathbb{Z}^{120}$,*

$$\|Mz\|_\infty \geq 10. \tag{9}$$

Proof. Suppose instead that $\|Mz\|_\infty \leq 9$. Integrality gives $|z_i| \leq z_i^2$ for every i, and therefore

$$z^T Mz \leq \sum_i |z_i| \, |(Mz)_i| \leq 9 \sum_i |z_i| \leq 9 \sum_i z_i^2.$$

Positive definiteness of $M - 9I$ gives the strict opposite inequality for nonzero z. Thus $\|Mz\|_\infty > 9$. Since Mz is integral, its infinity norm is at least ten. □

This is a lower bound, not a claim that ten is attained. More generally, if a symmetric integer matrix H has least eigenvalue $\alpha > 0$, the same comparison gives $\|Hz\|_\infty \geq \lceil \alpha \rceil$ for every nonzero integer z. In particular, a certificate that $H - kI$ is strictly positive definite for an integer k implies $\alpha > k$, and hence $\|Hz\|_\infty \geq k + 1$.

4 A 360-bit predecessor witness

Theorem 4.1 (Universal exact recovery)**.** *The map* (1) *is injective on $\mathbb{Z}^{120}$. Thus its reduced output and complete modulo-eight witness determine the original integer state uniquely.*

Proof. Suppose $T(d) = T(e)$ and $r(d) = r(e)$. Equal residues imply $d - e = 8z$ for some $z \in \mathbb{Z}^{120}$. Two real numbers with the same floor differ by less than one, so

$$\|QM(d - e)/D\|_\infty < 1.$$

The exact constants satisfy

$$73Q < D < 74Q. \tag{10}$$

Since $M(d - e)$ is integral, every coordinate has absolute value at most 73. Substituting $d - e = 8z$ gives $\|Mz\|_\infty \leq 9$. Lemma 3.2 forces $z = 0$, hence $d = e$. □

Equivalently, a nonzero z would imply $\|QM(8z)/D\|_\infty \geq 80Q/D > 1$, directly contradicting the same-floor bound. The proof is uniform over the integer domain. Existence for a valid record is supplied by the encoded predecessor.

Proposition 4.2 (Packing and restricted capacity minimum)**.** *The complete residue vector has an independent fixed-width binary representation of exactly 360 bits, and no shorter independent fixed-width representation can encode all such vectors.*

Proof. Define

$$R(d) = \sum_{i=0}^{119} (d_i \bmod 8) 8^{119-i}, \qquad 0 \leq R(d) < 8^{120} = 2^{360}. \tag{11}$$

This is positional base-eight notation, with three bits per digit. Every one of the 8^{120} residue vectors occurs, for example by choosing d in $\{0, \ldots, 7\}^{120}$. Any injective code for that full set into fixed b-bit strings must satisfy $2^b \geq 2^{360}$. The packing attains $b = 360$, or 45 bytes. □

The word *independent* is essential: this proposition represents the complete residue vector without using $T(d)$ to reduce its range. It does not prove that an arbitrary output-conditioned recovery witness needs 360 bits. It also does not say that all output/witness combinations are valid.

4.1 A concrete collision distinguished by the record

Let

$$d = (0, \dots, 0, 1, 0), \qquad e = (0, \dots, 0, 1, 5).$$

Because $M = 13I + A$ has diagonal entries 13 and off-diagonal entries in $\{0, 1\}$, every coordinate of Md and Me is nonnegative and at most $13 \cdot 5 + 1 \cdot 1 = 66$. Since $66Q < D$, both reduced outputs are zero. Their records are different: $R(d) = 8$ and $R(e) = 13$. Decoding with the respective records recovers the two different original states. The shared reduced output therefore represents a genuine ambiguity of the projection.

Proposition 4.3 (General sufficient condition)**.** *Let m, n be positive integers and let $H \in \mathbb{Z}^{m\times n}$ satisfy $\|Hz\|_\infty \geq k > 0$ for all nonzero $z \in \mathbb{Z}^n$. If a real number $\alpha > 0$ and a positive integer b satisfy $\alpha bk \geq 1$, then*

$$d \longmapsto \left(\lfloor \alpha H d \rfloor, d \bmod b\right)$$

is injective on $\mathbb{Z}^n$, with componentwise floor and modulo-b reduction.

Proof. Equal residues give a difference bz. If $z \neq 0$, its image has infinity norm at least $\alpha bk \geq 1$, whereas equal floors require this norm to be strictly less than one. □

This supplies a reusable proof pattern. Applying it to another graph or quantization rule requires establishing the corresponding separation and parameter inequalities.

5 A finite exact decoder

For a supplied output $y \in \mathbb{Z}^{120}$, let

$$a_i = \lceil Dy_i/Q \rceil, \qquad b_i = \lceil D(y_i + 1)/Q \rceil - 1. \tag{12}$$

The mathematical floor definition gives the exact equivalence

$$T(d) = y \quad \Longleftrightarrow \quad a \leq Md \leq b. \tag{13}$$

Every interval $[a_i, b_i] \cap \mathbb{Z}$ contains 73 or 74 integers. Its endpoint difference $b_i - a_i$ is 72 or 73.

5.1 Coordinate candidate sets

Write $z = Md$. From $d = Nz/h$ and (13), define

$$\ell_i = \frac{1}{h}\left(\sum_{N_{ij}\geq 0} N_{ij}a_j + \sum_{N_{ij}<0} N_{ij}b_j\right), \tag{14}$$

$$u_i = \frac{1}{h}\left(\sum_{N_{ij}\geq 0} N_{ij}b_j + \sum_{N_{ij}<0} N_{ij}a_j\right). \tag{15}$$

Every compatible predecessor satisfies $\ell_i \le d_i \le u_i$. The exact inverse certificate yields

$$u_i - \ell_i \le \frac{73}{h} \sum_j |N_{ij}| \le \frac{787597}{66625} < 12. \tag{16}$$

Set $L_i = \lceil \ell_i \rceil$ and $U_i = \lfloor u_i \rfloor$. For supplied residues $r_i \in \{0, \dots, 7\}$, form

$$\mathcal{D}_i = \{v \in \mathbb{Z} : L_i \le v \le U_i,\ v \equiv r_i \pmod 8\}. \tag{17}$$

Each set has at most two members: three congruent integers would span at least sixteen. A set may be empty, in which case the record is invalid.

Theorem 5.1 (Finite decoding)**.** *Enumerating $\prod_i \mathcal{D}_i$ and retaining precisely the vectors satisfying* (13) *terminates. A valid record has exactly one survivor. A completed search with no survivors proves that the record has no compatible predecessor.*

Proof. There are at most 2^{120} candidate leaves. Every compatible integer state lies in the product by construction. The exact constraints are equivalent to the supplied output, and Theorem 4.1 gives at most one survivor. For a valid encoded record its original state survives. □

5.2 Exact pruning and resource limits

The reference decoder uses row-interval propagation before branching. For a row i, let $S_i = \{j : M_{ij} \neq 0\}$. All coefficients M_{ij} for $j \in S_i$ are positive. For current candidate domains and each $j \in S_i$, a value $v \in \mathcal{D}_j$ can remain only if

$$a_i - \sum_{k \in S_i \setminus \{j\}} M_{ik} \max \mathcal{D}_k \le M_{ij} v \le b_i - \sum_{k \in S_i \setminus \{j\}} M_{ik} \min \mathcal{D}_k. \tag{18}$$

Removing values that violate this necessary condition preserves all valid solutions. Repeat until domains stop changing, or reject the current branch if any domain becomes empty. If ambiguity remains, choose a coordinate j with $|\mathcal{D}_j| = 2$, branch on its two remaining values, and apply propagation recursively in each branch. Every singleton leaf is re-encoded and compared exactly with the supplied (y, r); only matching leaves are retained. By Theorem 4.1, at most one leaf can match, so the search may return immediately on finding it. Invalid records are rejected only after all branches have been eliminated, unless a resource limit interrupts the search.

This procedure is finite without a resource cap. A configured search budget can stop it earlier; that outcome is explicitly unresolved, not invalid and not a guessed reconstruction. The natural n-coordinate extension can have 2^n leaves before pruning. At the fixed dimension 120 the cap is a concrete finite number, but it supplies no useful worst-case latency promise. Arithmetic costs also depend on the bit lengths of the input values.

5.3 Comparison with a specified independent-coordinate baseline

The intervals (16) also permit an independent-coordinate decoder when residues modulo twelve are supplied: two integers with the same residue differ by at least twelve, exceeding the interval width. Packing all 120 modulo-twelve residues requires 431 bits, since

$$2^{430} < 12^{120} < 2^{431}. \tag{19}$$

The joint modulo-eight construction uses 360 bits, a 71-bit witness reduction relative to this baseline. Byte-aligned storage changes from 54 to 45 bytes. This is a comparison of specified witness constructions, not a proof that twelve is optimal among all independent coding methods, nor a total-storage or runtime benchmark.

6 Finite histories and explicitly encoded messages

Theorem 6.1 (Finite-history recovery)**.** *Let $n \geq 0$ and let $d^{t+1} = T(d^t)$ for $0 \leq t < n$. The terminal state d^n together with the ordered witnesses $r(d^0), \ldots, r(d^{n-1})$ uniquely determines every state $d^0, \ldots, d^n$.*

Proof. For $n = 0$ the terminal state is already the only state. For $n > 0$, apply Theorem 4.1 to d^n and $r(d^{n-1})$ to recover d^{n-1}. Repeat backwards, or apply induction to the remaining trajectory. Each step has a compatible predecessor because it was recorded from the stated trajectory. □

The construction uses n witnesses, with a packed payload of $360n$ bits. Terminal-state storage and framing are additional. A transition caused by an unrecorded external update is outside the theorem. Ordering matters because each witness refers to the predecessor of a particular transition. Absolute timestamps and external controls require additional record fields when an application needs them.

Proposition 6.2 (Finite-message composition)**.** *Every finite byte string has an explicit injective encoding into a network state. Combining this encoding with a finite witnessed trajectory permits exact recovery of the byte string.*

Proof. For a byte string m of length L, define

$$J(m) = 256^L + \mathrm{value}_{256}(m), \qquad E(m) = (J(m), 0, \ldots, 0). \tag{20}$$

Equivalently, prepend byte `01` and interpret the resulting bytes as a big-endian unsigned integer. The intervals $[256^L, 2 \cdot 256^L)$ for distinct lengths are disjoint. Within a length, positional notation distinguishes the strings. Removing the marker recovers the bytes, including leading zero bytes and the empty string. Recover the initial network state by Theorem 6.1, then invert E. □

This statement applies to an explicitly encoded finite record. Its meaning, coordinate frame, units, and other interpretation must be specified by that record's codec. For example, an exact record of an approximation reproduces the recorded approximation.

7 Storage and interoperability

7.1 The agreed binary witness

The reference witness is the integer R in (11), stored as exactly 45 unsigned big-endian bytes. Coordinate zero supplies the most significant three bits. Thus residues $(1, 0, \ldots, 0)$ produce hexadecimal byte `0x20` (decimal 32) followed by 44 zero bytes (`0x00`); $(0, \ldots, 0, 1)$ produce 44 zero bytes followed by `0x01`. The packing identifier, with the decimal digit zero in its coordinate field, is `MOD8_COORDINATE_0_FIRST_BE/1`.

A later working checkpoint used the alternative $R_{\mathrm{LE}} = \sum_i r_i 8^i$, stored as 45 little-endian bytes. Both conventions are reversible, but their bytes cannot be silently interchanged. The supplied adapter recovers the residues and repacks them under an explicit identifier. Because the digits have three bits, conversion is generally not just byte reversal. Existing source records retain their original schemas.

7.2 Portable state values and history framing

The consolidated `OMEGA_PAPER_IX_RECORD/1` document contains the model identifier, graph digest, packing identifier, 120 output-coordinate strings, and the witness as 90 lowercase hexadecimal characters. The coordinate strings use canonical signed decimal notation. This avoids silent rounding when a JSON consumer implements numeric values with limited precision; RFC 8259 discusses the relevant interoperability limits [11]. The parser rejects duplicate fields, non-finite constants, and malformed coordinates.

`OMEGA_PAPER_IX_HISTORY/1` additionally specifies a transition count, terminal vector, and chronological witness list of that exact length. The decoder consumes the witnesses in reverse chronological order. Empty histories are allowed. Large-integer conversion uses decimal chunks rather than relying on an interpreter's optional decimal-digit limit.

Hexadecimal, direction-symbol, and letter-group displays occupy more bytes than the packed witness. The 45-byte claim counts only the binary payload. If graph identifiers, constants, or other rules must be transmitted, their cost is included in a complete application record. Uniqueness does not by itself authenticate a record: a changed witness can identify another valid input for the same output.

7.3 Optional ordered displays

A fixed six-symbol alphabet can display the integer R in 140 base-six positions, preserving leading zeros, because $6^{139} < 2^{360} \leq 6^{140}$. One implemented interface labels these symbols with directions and ordered three-letter groups. Such labels preserve information through their order, not through a shared numerical sum or the final endpoint of a drawn path. They are optional interfaces to the same binary witness and do not enter the recovery proof.

8 Exact computation and implementation evidence

The consolidated reference sources were replayed on 5 November 2026 under Python 3.12.14. The geometric minor enumerator was compiled with `g++` 14.2.0 and C++17. Corresponding deterministic reports from normal and optimized Python modes agree byte for byte. Elapsed-time logs are stored separately; no comparison of machine performance is inferred from them.

The core suite checks signed bin endpoints, same-output examples, invalid records, exact re-encoding, and explicit budget exhaustion. In the 1,109 valid core cases, propagation resolved decoding at one search node; this observation is not a general runtime bound. Separate rejection cases exercise branching. The portable-format checks include integers exceeding 4,300 decimal digits, verifying the exact file boundary rather than only residue extraction.

For the geometric certificate, complete exact coefficients through degree seven, the permanent tail, and the cover symmetries were freshly replayed in both modes during consolidation. This revision also cross-checked all eight low-degree coefficients with the shared-prefix elimination method

Check	Cases per mode
Core, complete 120-coordinate reconstruction	1,109
Directional interface, complete reconstruction	153
Packing conversion against positional arithmetic	960
Portable records with large signed integers	5
Finite history records, including empty histories	15
Transitions reconstructed within those histories	25
Malformed consolidated documents rejected	15

Table 1: Executed implementation checks. Repeated execution modes and overlapping suites do not create additional distinct test inputs.

described in Appendix A. That implementation passed 144 small signed matrix controls against direct rational determinant enumeration, and its permanent routine passed 15 direct matching-enumeration controls. The full coefficient and control reports agree in normal and optimized Python modes. Appendix A states the conventional argument linking the calculations to the research interval. The expanded standalone checker in Appendix B also produced identical result bytes in both modes. These checks strengthen reproduction; they do not narrow the interval.

The supplied Lean file verifies arithmetic comparisons and conditional capacity implications. It does not formalize the complete graph, geometry, decoder, and history proof. No Lean or Julia runtime was available for a fresh execution during this consolidation. The present evidence is a conventional proof supported by exact finite computation, with partial formalization retained separately.

9 The distinct minimum-width problem

For $y \in \mathbb{Z}^{120}$ define the output fiber $\mathcal{F}_y = \{d \in \mathbb{Z}^{120} : T(d) = y\}$. A fixed-width recovery code conditioned on y must distinguish all its members. Let

$$F_{\max} = \max_y |\mathcal{F}_y|, \qquad \ell^* = \lceil \log_2 F_{\max} \rceil . \tag{21}$$

The explicit witness makes these sizes uniformly bounded, so the maximum is well defined. A sufficiently large fixed code exists in principle by agreeing on an enumeration of each finite fiber and storing its index. Efficiently computing that index is a separate algorithmic requirement.

Theorem 9.1 (Separate output-conditioned capacity bounds)**.** *For the exact operator* (4) *on* $\mathbb{Z}^{120}$*,*

$$2^{306} < F_{\max} < 2^{352}, \qquad 307 \le \ell^* \le 352. \tag{22}$$

Proof. Appendix A proves an exact reduction to box points modulo $M\mathbb{Z}^{120}$. Averaging over those classes gives the strict lower bound. A packing argument, an exact coordinate cover, and a certified projected zonotope-volume upper estimate give the strict upper bound. □

The interval locates an integer optimum; it does not make the 360-bit construction inconsistent. Proposition 4.2 encodes every complete residue vector independently. Equation (21) permits a different witness exploiting compatibility with the supplied output. Finding the exact optimum and implementing useful exact ranking and unranking remain continuing research.

Record or bound	Bits	Meaning
Specified independent modulo-twelve vector	431	Sufficient baseline
Implemented joint modulo-eight vector	360	Explicit exact codec
General output-conditioned sufficient capacity	352	In-principle index
General necessary worst-case width	307	Lower bound

Table 2: Different coding questions and constructions. Output and metadata are additional to every witness count.

10 Relation to existing methods

Maclaurin, Duvenaud, and Adams [3] reverse learning dynamics by retaining auxiliary finite-precision information. This establishes an important precedent for witnessed history reconstruction. Paper IX supplies a different, explicitly specified integer map and a fixed residue witness; it does not show an improvement in training memory or performance.

Calderbank, Daubechies, Sweldens, and Yeo [4] construct integer-to-integer wavelet transforms, including rounding-compatible lifting methods. Such transforms arrange invertibility through their transform structure. Here the chosen flooring map is kept and accompanied by a separate record. Comparisons must account for the respective outputs and all retained information rather than comparing witness lengths alone.

Mayekar, Suresh, and Tyagi [5] analyze communication-efficient mean estimation with decoder side information. Ordentlich and Erez [6] use nested lattices and recovered integer combinations in lossy coding of correlated Gaussian sources; Zamir, Shamai, and Erez [7] develop a broader structured binning framework. These works provide context for modular information and joint decoding, with objectives and source assumptions different from the all-input exact theorem here.

The uniform-cover inequality and zonotope volume formula used in the capacity bound are established tools [8, 9, 10]. The fixture-specific automorphisms, coefficient calculations, and exact parameter comparisons specialize those tools to the present network. This targeted comparison does not establish historical priority for the construction.

11 Continuing research

The first open problem is to determine the exact $F_{\max}$ or integer ℓ^* in (21). The proof of the explicit modulo-eight construction does not require solving this problem. The second is to improve decoding and, for smaller output-conditioned witnesses, exact ranking and unranking. Tractable input classes and worst-case guarantees should be identified separately from example timings.

A complete formal development would connect the graph construction, integer matrix certificates, geometric volume argument, and recovery theorems within one proof assistant. Other graphs and quantization rules can be investigated through Proposition 4.3, with new separation certificates and explicit parameter conditions.

Application evaluation requires conventional baselines and a complete count of stored or transmitted output, witness, metadata, runtime, and working memory. Preserving a finite witnessed trajectory is not by itself a compression advantage over storing its initial state and recomputing it. The relevant tradeoffs depend on the workload and access requirements.

12 Conclusion

For the specified 600-cell operator, the reduced output and a 45-byte modulo-eight record uniquely determine every integer predecessor. Exact matrix certificates, integer separation, and quantization bounds establish the guarantee. A finite decoder realizes it, and backward induction extends it to finite histories with retained terminal states and ordered witnesses. The explicit record and its interpretation make exact reproduction a checkable mathematical statement. Smaller records, faster reconstruction, and demonstrated application benefits remain distinct research objectives.

Data, software, and provenance

This draft is accompanied by `Paper_IX_Draft_0_6_Source_and_Certificates.zip`. It contains the editable LaTeX source, the standalone checker, the preserved reference codec, the geometric verifiers, the versioned format adapter, actual execution reports, and SHA-256 manifests. Reproduction commands are given in Appendix C. Hashes identify bytes; they do not replace mathematical checking or independent review.

The draft develops the author's earlier Paper IX manuscript using the 5 November 2026 consolidated foundation. The corrected degree-eleven permanent coefficient in Appendix A agrees with the executable certificate; a differing entry in a prior prose table was a transcription error. The reproduced upper volume is unchanged.

Draft 0.5 records responses to a supplied manuscript audit and a further orbit/minor checker. The latter required an indentation repair and corrected subset-count guards before execution. Its verified revision agrees with the coefficient table, while distinguishing positive-multiplicity directions from the zero-multiplicity directions retained by the reference enumeration. The source archive contains the corrected implementation, actual reports, and an audit-response record. Supplied execution claims are not treated as independent runs by the author or as peer review.

Draft 0.6 adds two original images created by ChatGPT. The first is computed from the exact graph fixture. The second uses a fully specified two-dimensional lattice analogue to illustrate packing and labels the actual 120-dimensional inequalities separately. The source archive includes the figure-generation program, exact input data, validation report, and vector and raster exports. Floating-point calculations are used only for drawing and viewing transformations. The mathematical checkers and the 360-bit construction and 307–352-bit bounds are unchanged.

The DOI on the title page is included as designated by the author. Public repository metadata for that identifier were not confirmed during draft preparation. This document does not report a completed repository deposit.

Acknowledgment and preparation disclosure

The OMEGA research direction is Matthew Alan Newman's. Mathematical exposition, software preparation, consolidation, and source comparison were AI-assisted. The author is responsible for the claims in a submitted version. No independent peer review or complete proof-assistant certification is represented as completed.

A Proof of the separate 307–352-bit bounds

A.1 Finite-group reduction and phase realizability

Let $L = M\mathbb{Z}^{120}$ and $G = \mathbb{Z}^{120}/L$, of order Δ in (7). Put $B = \{0, \dots, 73\}^{120}$ and define

$$H(c) = |\{u \in B : [u] = c\}|, \qquad c \in G. \tag{23}$$

By (12), every output fiber is a lattice intersection with a product of 73- or 74-integer intervals. It is contained in a translate of B, giving $\max_y |\mathcal{F}_y| \le \max_c H(c)$.

For the reverse direction, fix an arbitrary $a \in \mathbb{Z}^{120}$. Let

$$g_0 = \gcd(Qh, D) = 8000, \qquad \sigma = D - 73Q = 183666691831206. \tag{24}$$

The exact inequalities $0 < g_0 \le \sigma < Q$ hold. For each coordinate choose $\rho_i = Qa_i \bmod g_0$, with $0 \le \rho_i < g_0$, and solve

$$Qhk_i \equiv \rho_i - Qa_i \pmod{D}. \tag{25}$$

This is solvable because its right side is divisible by g_0; after division by g_0, the coefficient is invertible modulo D/g_0. Set $b = a + hk$ and $y_i = (Qb_i - \rho_i)/D$. Then $Qb_i = Dy_i + \rho_i$. Both b_i and $b_i + 73$ lie inside the half-open bin for y_i, because $\rho_i < g_0 \le D - 73Q$. The preceding integer is excluded by $\rho_i < Q$, and the following one by $74Q > D$. The bin is exactly $\{b_i, \dots, b_i + 73\}$.

Moreover, $hk = MNk \in L$. Translation by hk therefore gives a bijection between $L \cap (a + B)$ and $L \cap (b + B)$. Every translated full-box lattice count is consequently an actual output-fiber count. Thus

$$F_{\max} = \max_{c \in G} H(c). \tag{26}$$

The sets in (23) partition the 74^{120} box points, so $F_{\max} \ge \lceil 74^{120}/\Delta \rceil$. Exact comparison gives

$$2^{306}\Delta < 74^{120} < 2^{307}\Delta, \tag{27}$$

proving $\ell^* \ge 307$. Since $M\mathbf{1} = 25\mathbf{1}$, every $d \in \mathbb{Z}^{120}$ and $t \in \mathbb{Z}$ satisfy the exact shift identities

$$C(d + tD\mathbf{1}) = Cd + 25tQ\mathbf{1}, \qquad T(d + tD\mathbf{1}) = T(d) + 25tQ\mathbf{1}.$$

Translation by $tD\mathbf{1}$ is a bijection from $\mathcal{F}_y$ to $\mathcal{F}_{y+25tQ\mathbf{1}}$, with inverse translation by $-tD\mathbf{1}$. Choosing t sufficiently large places an entire finite maximizing fiber inside $\mathbb{N}_0^{120}$, so the same maximum holds there. This argument does not establish the same lower bound on a fixed bounded cube.

A.2 Packing into a continuous zonotope

Define

$$K = [0, 73]^{120} + M[0, 1]^{120}. \tag{28}$$

Fix a class c, choose a representative u_0, and write each counted box point uniquely as $u = u_0 + Mz$ with $z \in \mathbb{Z}^{120}$. The half-open cubes $z + [0, 1)^{120}$ are disjoint. Their images under $x \mapsto u_0 + Mx$ are also disjoint, each has volume Δ, and every image lies in $u + M[0, 1]^{120} \subseteq K$. Therefore

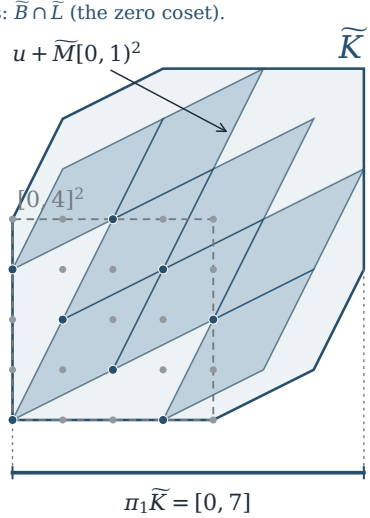
$$H(c)\Delta \le \mathrm{vol}_{120}\, K. \tag{29}$$

This converts the count to the volume of disjoint parallelotopes; it does not identify a discrete set with a continuous body of equal volume. Figure 2 illustrates this packing mechanism in an exact two-dimensional analogue and summarizes the actual cover inequality below.

Packing and the coordinate-cover bound

An exact 2D analogue

Blue points: $\widetilde{B} \cap \widetilde{L}$ (the zero coset).



Columns of $\widetilde{M}$: $(2,1)^T$, $(1,2)^T$; $\det \widetilde{M} = 3$.
Eight half-open cells: total area $24 \le \text{area}(\widetilde{K}) = 43$.

The panel is not a computed view of the 120D body or its 13D projections.

Image created by ChatGPT

The actual 120-dimensional statement

$B = \{0, \ldots, 73\}^{120}$

$L = M\mathbb{Z}^{120}, \quad \Delta = \det M$

$c \in G = \mathbb{Z}^{120}/L$

$H(c) = |B \cap (u_0 + L)|, \quad [u_0] = c$

$F_{\max} = \max_{c \in G} H(c)$

$K = [0,73]^{120} + M[0,1]^{120}$

$H(c)\Delta \le \text{vol}_{120}(K)$

$V(73) = \text{vol}_{13}(\pi_W K)$

120 blocks; an exact 13-cover.

$(F_{\max}\Delta)^{13} \le V(73)^{120}$

$307 \le \ell^* \le 352$

Figure 2: Packing and projection, illustrated using $\widetilde{M} = \left(\begin{smallmatrix} 2 & 1 \\ 1 & 2 \end{smallmatrix}\right)$, $\widetilde{B} = \{0, \ldots, 4\}^2$, and $\widetilde{L} = \widetilde{M}\mathbb{Z}^2$. Eight points of $\widetilde{B} \cap \widetilde{L}$ give disjoint half-open cells of area three inside $\widetilde{K} = [0,4]^2 + \widetilde{M}[0,1]^2$, whose area is 43. Its first-coordinate projection is $[0,7]$. Cell boundaries are drawn with closed outlines for visibility. This is not a computed view of the actual 120-dimensional body or its 13-dimensional projections; the right panel states the actual inequalities of this appendix. Image created by ChatGPT.

A.3 The exact coordinate cover

Take $W = \{0, 33, 34, \dots, 44\}$, the closed neighborhood of vertex zero. Using the unit-quaternion representation of the vertices, the checker constructs all 120 left-multiplication permutations. It verifies that each is a graph automorphism, that the projected generator multisets agree in transported coordinate order, and that the translated copies of W contain every coordinate exactly thirteen times. If P_s is the permutation matrix of such an automorphism, $P_s M = M P_s$ and both coordinate cubes are invariant under P_s. Thus $P_s K = K$, and its restriction to the corresponding coordinate subspaces is an isometry. In particular,

$$\mathrm{vol}_{13}(\pi_{g_s(W)} K) = \mathrm{vol}_{13}(\pi_W K).$$

The projected-generator checks verify this symmetry on the exact fixture.

The Bollobás–Thomason uniform-cover inequality [8], in the form of [9, Theorem 1.1, equation (1.5)], says that if coordinate sets W_s form an exact k-cover and a compact full-dimensional body is the closure of its interior, then $\mathrm{vol}(K)^k \le \prod_s \mathrm{vol}(\pi_{W_s} K)$. These hypotheses hold for the zonotope (28). Let $V = \mathrm{vol}_{13}(\pi_W K)$. Equality of the projected volumes gives

$$(F_{\max}\Delta)^{13} \le (\mathrm{vol}_{120}\, K)^{13} \le V^{120}. \tag{30}$$

A.4 Exact coefficients and a permanent tail

The maximal-minor formula for zonotope volume [10] gives

$$V(t) = \mathrm{vol}_{13}\big(t[0,1]^{13} + \pi_W M[0,1]^{120}\big) = \sum_{r=0}^{13} a_r t^{13-r}, \tag{31}$$

$$a_r = \sum_{\substack{I \subseteq W \\ |I|=r}} \sum_{\substack{J \subseteq \{0,\dots,119\} \\ |J|=r}} |\det M_{I,J}|. \tag{32}$$

For the nonnegative matrix M, determinant expansion gives $|\det B| \le \mathrm{perm}(B)$. Let p_r be the sum of these permanents over the same submatrices; then $a_r \le p_r$.

For the permanent sum, process the 120 columns one at a time. If $D_j(T)$ is the total weight of matchings covering precisely the row set T after the first j columns, then

$$D_{j+1}(T) = D_j(T) + \sum_{i \in T} M_{ij} D_j(T \setminus \{i\}). \tag{33}$$

Initialize $D_0(\varnothing) = 1$ and other states to zero. Leaving the next column unused or matching it to one distinct row are disjoint exhaustive cases. Summing $D_{120}(T)$ by $|T| = r$ yields p_r, using 2^{13} exact integer states.

All eight low-degree coefficients are complete minor sums. The local stabilizer of vertex zero has order 120; its row-subset orbit counts for $r = 0, \dots, 7$ are $(1, 2, 4, 8, 15, 22, 30, 30)$. The new checker constructs the local permutations using exact inner products in $\mathbb{Z}[\phi]$ and lifts each to a verified automorphism of the full graph. A four-vector Gram determinant is $32 - 16\phi \neq 0$, establishing spanning. Color refinement shows that fixing an ordered local triangle fixes its twelve vertices, and fixing W pointwise fixes all 120 vertices. The 120 possible ordered triangle images therefore bound the full stabilizer from above, matching the 120 constructed elements. The raw neighbor vertices lie in the affine hyperplane $x_0 = -\phi/2$; their centered vertex figure lies in $x_0 = 0$.

r	Exact a_r used	Permanent p_r used
0	1	–
1	325	–
2	45408	–
3	3647440	–
4	188983720	–
5	6697090056	–
6	167581390636	–
7	3007006391716	–
8	–	82326531807696
9	–	879734614473680
10	–	6510322192690880
11	–	31533042290406720
12	–	89385221732384160
13	–	111664804452677280

Table 3: Exact low-degree coefficients and coefficientwise upper tail for the 13-coordinate projected volume. An absent entry is not asserted zero.

For a row representative I, group identical nonzero restricted columns into vectors $v_1, \dots, v_m$ with positive multiplicities $\mu_1, \dots, \mu_m$. A minor using two copies of an identical column vanishes. Consequently its row contribution is exactly

$$\sum_{|J|=r} |\det M_{I,J}| = \sum_{1 \le j_1 < \cdots < j_r \le m} \mu_{j_1} \cdots \mu_{j_r} |\det(v_{j_1}, \dots, v_{j_r})|.$$

The contribution is constant on each row orbit because each local automorphism also permutes all 120 columns. Multiplication by orbit sizes recovers (32) without sampling.

Two enumeration conventions give different subset counts. The retained reference implementation also inserts coordinate-axis directions with zero multiplicity. They contribute zero to every weighted sum. Removing them reduces the counts as follows; neither convention counts repeated original columns as distinct generator directions.

r	Directions retained	Row orbits	Representative subsets	Orbit-weighted subsets
6	Reference, including zero weights	30	5117618	290644970
6	Positive weights only	30	4800238	267471890
7	Reference, including zero weights	30	45111870	2733293660
7	Positive weights only	30	40449768	2474330048

Table 4: Exact combination counts under the two compression conventions. These are candidate-subset counts, not counts of nonzero determinants or timing measurements. Both conventions reproduce the same a_r.

The new implementation shares fraction-free Bareiss elimination among combinations with a common prefix. For a pivot p, previous pivot q, and remaining coordinate c, a candidate vector is updated by $v'_c = (p v_c - v_{\mathrm{piv}} p_c)/q$; every division is checked exact. Once only two-vector candidates (x_a, y_a) remain, Sylvester's identity gives each remaining determinant magnitude as $|x_a y_b - y_a x_b|/|p_*|$, where p_* is the last pivot used to obtain those two-vectors. Weighted cross products are summed before the final exact division. Dependent prefixes contribute zero and may be skipped. The resulting

coefficients agree with the retained verifier and with the direct small-matrix controls described in Section 8.

Since $73 \geq 0$, coefficientwise domination yields

$$V = V(73) \leq U := \sum_{r=0}^{7} a_r 73^{13-r} + \sum_{r=8}^{13} p_r 73^{13-r} \\ = 58067516542393048415542654. \tag{34}$$

The exact integer comparison

$$U^{120} < (2^{352}\Delta)^{13} \tag{35}$$

together with (30) proves $F_{\max} < 2^{352}$.

The partial volume through degree seven is

$$L_7 = 57869157529977646724169246, \qquad L_7^{120} > (2^{351}\Delta)^{13}.$$

Thus refining the remaining coefficients of this same equal-volume cover cannot establish a 351-bit upper bound by this projection inequality. This does not prove that the true optimum is 352.

A.5 Arithmetic safety and the proof boundary

The retained native minor enumerators use signed 128-bit integers, with input and exact-division checks. For their dimensions at most eight, a conservative determinant bound is $k!13^k \leq 8!13^8 < 2^{45}$; this controls the fraction-free products in their delivered calculation. The new shared-prefix kernel accepts dimensions at most seven and explicitly checks every signed 128-bit addition, subtraction, multiplication, and division, including zero divisors and division remainders. Both complete coefficient runs finished without overflow or nonexact division. A failed guard aborts the calculation instead of issuing a certificate. Its small signed-matrix controls compare against rational Gaussian elimination with one determinant per subset. Python calculations use arbitrary-precision integers.

The Lean capacity statements take the actual packing inequality and supplied arithmetic data as hypotheses or definitions. They do not establish the graph-to-volume connection within Lean. The computation above is part of a conventional proof using the cited geometric theorem.

B A standalone exact checker for the core theorem

The following complete program regenerates the graph, verifies all 120 positive leading determinants of $M - 9I$, constructs the exact inverse numerator from (8), and recomputes the permanent coefficients by (33). It checks the lower capacity comparison, assembles L_7 and U from the supplied $a_0, \ldots, a_7$ and recomputed permanent tail, and checks both upper-threshold comparisons. The low-degree minor coefficients are explicitly supplied inputs to this program: their recomputation is performed by the companion orbit/minor checker and retained geometric verifiers. The global coordinate cover is also checked separately. It uses Python's standard library and explicit failure checks, so optimized execution does not disable its validation. Its output includes the leading determinants and its actual source hash. For exact executable bytes, use the source archive rather than copying a line-wrapped listing from the PDF.

The fixture digest and serialization contract are listed in Appendix C; the program defines the exact JSON fields.

```
#!/usr/bin/env python3
"""Exact core certificates, permanent tail, and conditional capacity arithmetic.

Python 3.10+, standard library only. No assertions, floating point, external
data, or numerical eigensolver. The low-degree absolute-minor coefficients
are supplied here, not recomputed. The companion orbit/minor checker and
retained geometric verifiers compute them separately. This is not an exact
maximum-fiber calculation or a practical speed claim.
"""
from hashlib import sha256
from itertools import combinations, permutations, product
from math import gcd
from pathlib import Path
import json

Q=339949771344778
D=25000000000000000
H=4948372000
PIN='40bc6a1d52efab3d75cf343e65ac06b314f9c9c375fc02bf6d45bf6bb21f9529'

def require(ok, message):
    if not ok:
        raise ArithmeticError(message)

def graph():
    vertices=set()
    for i in range(4):
        for s in (-1,1):
            v=[(0,0)]*4
            v[i]=(2*s,0)
            vertices.add(tuple(v))
    for signs in product((-1,1),repeat=4):
        vertices.add(tuple((s,0) for s in signs))
    even=[p for p in permutations(range(4))
          if sum(p[i]>p[j] for i in range(4)
                 for j in range(i+1,4))%2==0]
    for a,b,c in product((-1,1),repeat=3):
        v=((0,0),(a,0),(0,b),(-c,c))
        vertices.update(tuple(v[i] for i in p) for p in even)
    vertices=sorted(vertices)
    neighbors=[[] for _ in vertices]
    for i,j in combinations(range(len(vertices)),2):
        x=y=0
        for (a,b),(c,d) in zip(vertices[i],vertices[j]):
            u,v=a-c,b-d
            x+=u*u+v*v
            y+=2*u*v+v*v
        if (x,y)==(8,-4):
            neighbors[i].append(j)
            neighbors[j].append(i)
    fixture={
        'coordinate_rule':
            'vertex coordinate is (a+b*phi)/2 for pair [a,b]',
        'neighbors':neighbors,
        'schema':'OMEGA_600CELL_GRAPH_FIXTURE/1',
        'vertex_order':
            'Python lexicographic order of tuples of four integer pairs',
        'vertices':vertices}
    raw=(json.dumps(fixture,sort_keys=True,separators=(',',':'))+'\n').encode()
    require(sha256(raw).hexdigest()==PIN,'graph identity')
    require(len(vertices)==120 and all(len(v)==12 for v in neighbors),
            'dimension and degree')
    return neighbors

```

```
def bareiss_positive(a):
    a=[list(row) for row in a]
    n=len(a)
    previous=1
    minors=[]
    for k in range(n):
        pivot=a[k][k]
        require(pivot>0,'positive leading determinant')
        minors.append(pivot)
        for i in range(k+1,n):
            for j in range(k+1,n):
                num=a[i][j]*pivot-a[i][k]*a[k][j]
                value,remainder=divmod(num,previous)
                require(remainder==0,'exact Bareiss division')
                a[i][j]=value
            a[i][k]=0
        previous=pivot
    return minors

def multiply_M(a,neighbors):
    return [[13*a[i][k]+sum(a[j][k] for j in neighbors[i])
             for k in range(120)] for i in range(120)]

def polynomial_product(a,b):
    c=[0]*(len(a)+len(b)-1)
    for i,x in enumerate(a):
        for j,y in enumerate(b):
            c[i+j]+=x*y
    return c

def permanent_coefficients(matrix):
    """All rectangular minor permanent sums by descending-mask updates."""
    m=len(matrix)
    require(m>0 and all(len(row)==len(matrix[0]) for row in matrix),
            'rectangular matching matrix')
    require(all(type(x) is int and x>=0 for row in matrix for x in row),
            'nonnegative integer matching weights')
    dp=[1]+[0]*((1<<m)-1)
    for j in range(len(matrix[0])):
        nz=[(1<<i,matrix[i][j]) for i in range(m) if matrix[i][j]]
        for mask in range((1<<m)-1,-1,-1):
            value=dp[mask]
            if value:
                for bit,weight in nz:
                    if not mask&bit:
                        dp[mask|bit]+=value*weight
    coeff=[0]*(m+1)
    for mask,value in enumerate(dp):
        coeff[mask.bit_count()]+=value
    return coeff

def verify():
    neighbors=graph()
    M=[[13 if i==j else int(j in neighbors[i])
        for j in range(120)] for i in range(120)]
    positive=bareiss_positive([
        [M[i][j]-9*int(i==j) for j in range(120)]
        for i in range(120)])
    determinant=bareiss_positive(M)[-1]
    delta=2**80*5**27*11**36*13**25*41**9*211**4
    require(determinant==delta,'exact determinant')
    f=[1]
    for factor in ([[-r,1] for r in (10,11,13,16,25)]
                   +[[211,-32,1],[205,-30,1]]):
```

```
        f=polynomial_product(f,factor)
    require(f[0]==-5*H,'annihilator constant')
    g=[[f[-1]*int(i==j) for j in range(120)]
       for i in range(120)]
    for coefficient in reversed(f[1:-1]):
        g=multiply_M(g,neighbors)
        for i in range(120):
            g[i][i]+=coefficient
    mg=multiply_M(g,neighbors)
    require(all(mg[i][j]==5*H*int(i==j)
                for i in range(120) for j in range(120)),
            'annihilating polynomial identity')
    require(all(v%5==0 for row in g for v in row),'integer inverse numerator')
    N=[[v//5 for v in row] for row in g]
    mn=multiply_M(N,neighbors)
    require(all(mn[i][j]==H*int(i==j)
                for i in range(120) for j in range(120)),
            'exact inverse identity')
    norm=max(sum(abs(v) for v in row) for row in N)
    require(norm==801320608 and 73*norm<12*H,'inverse interval width')
    require(73*Q<D<74*Q and 80*Q>D,'quantization inequalities')
    require(8**120==2**360,'modulo-eight capacity')
    require(2**430<12**120<2**431,'modulo-twelve capacity')
    require(0<gcd(Q*H,D)<=D-73*Q<Q,'phase hypotheses')
    require(2**306*delta<74**120<2**307*delta,'averaging thresholds')
    W=[0]+list(range(33,45))
    require(sorted([0]+neighbors[0])==W,'closed neighborhood W')
    permanent=permanent_coefficients([M[i] for i in W])
    require(permanent[8:]==[
        82326531807696,879734614473680,6510322192690880,
        31533042290406720,89385221732384160,111664804452677280],
        'recomputed permanent tail')
    supplied_a=[1,325,45408,3647440,188983720,6697090056,
                167581390636,3007006391716]
    L7=sum(a*73**(13-r) for r,a in enumerate(supplied_a))
    U=L7+sum(permanent[r]*73**(13-r) for r in range(8,14))
    require(L7==57869157529977646724169246,'partial volume assembly')
    require(U==58067516542393048415542654,'upper volume assembly')
    require(U**120<(2**352*delta)**13,'352-bit threshold arithmetic')
    require(L7**120>(2**351*delta)**13,'same-cover 351-bit obstruction')
    return {
        'schema':'OMEGA_PAPER_IX_CORE_CERTIFICATE/1','status':'PASS',
        'graph_sha256':PIN,'dimension':120,'degree':12,
        'M_minus_9I_positive_leading_minors':len(positive),
        'positive_leading_determinants':[str(v) for v in positive],
        'inverse_denominator':H,'inverse_row_norm_numerator':norm,
        'determinant_M':str(delta),'witness_bits':360,
        'recomputed_permanent_coefficients':permanent,
        'supplied_absolute_minor_coefficients_not_recomputed':supplied_a,
        'partial_volume_L7':str(L7),'upper_volume_U':str(U),
        'threshold_352_arithmetic_passes':True,
        'same_cover_351_obstruction_arithmetic_passes':True,
        'global_cover_checked_by_this_script':False,
        'low_degree_coefficients_recomputed_by_this_script':False,
        'source_sha256':sha256(Path(__file__).read_bytes()).hexdigest()}

if __name__=='__main__':
    print(json.dumps(verify(),indent=2,sort_keys=True))
```

C Reproduction and source inventory

The accompanying source archive preserves original executable sources and reports separately from newly generated evidence. From its root, the main commands are:

```
python3 core_certificate_check.py > core_new.json
python3 -O core_certificate_check.py > core_new_optimized.json
python3 verify_orbit_minor_sums.py --cpp > orbit_new.json
python3 -O verify_orbit_minor_sums.py --cpp > orbit_new_optimized.json
python3 check_minor_kernel_controls.py > controls_new.json
python3 render_figures.py
python3 reproduction/run_reference_checks.py \
  --output-dir new_checks/reference
python3 reproduction/verify_consolidation.py \
  --output-dir new_checks/interchange_normal
python3 -O reproduction/verify_consolidation.py \
  --output-dir new_checks/interchange_optimized
```

The reference replay uses temporary copies of the source directories so that original reports are not overwritten. The geometric stages additionally require a C++17 compiler and can take several minutes. The output reports record completed commands, exit status, actual elapsed times, and hashes. The new orbit checker needs only the Python standard library in its default mode, which recomputes a_0 through a_5 and explicitly labels a_6, a_7 as supplied. Its `--cpp` mode compiles the embedded checked C++17 kernel and recomputes all eight coefficients. Alternatively, `--max-r 7` evaluates all degrees using Python. The local checker does not replace the separately verified global cover or packing proof. The optional figure-generation command requires Matplotlib and NumPy; the figure report records the versions used. It checks the local graph labels and edges and the exact two-dimensional packing data, then writes PDF, SVG, and PNG images under `figures/`. The original mathematical verification commands do not require either drawing library.

The pinned fixture digest is

`40bc6a1d52efab3d75cf343e65ac06b314f9c9c375fc02bf6d45bf6bb21f9529`

The serialization is JSON with sorted keys, compact separators, and one terminal newline, with the exact fields defined by the program. The matrix premises checked here support the conventional proof in Sections 3–6; the program does not enumerate all integer inputs or determine $F_{\max}$.

The core encoder/decoder and display adapter are `omega_indicator.py` and `omega_directional.py`, under `reproduction/reference_codec/`. Geometric verifiers are under `reproduction/reference_bounds/`; the portable adapter is `reproduction/paper9_records.py`. Its format is specified under `specification/`.

The preserved core source has SHA-256

`fba18e7dc2a652187e4b89963f4904093e789e644c3e0e88a69671008784698a`

The baseline graph/matrix source has SHA-256

`57100e240ba7d1a8c10c133e51937461cf6b9b0cb1ef1602671095bd4375917b`

The archive manifest supplies the remaining source and result hashes. Corresponding normal/optimized reports are compared as bytes; runtime log agreement is not required. The old prose checksum table and corrected coefficient transcription are documented in the consolidation notes.

References

[1] H. S. M. Coxeter. *Regular Polytopes*, 3rd edition. Dover Publications, New York, 1973.

[2] E. H. Bareiss. Sylvester's identity and multistep integer-preserving Gaussian elimination. *Mathematics of Computation* 22(103), 565–578, 1968. doi:10.1090/S0025-5718-1968-0226829-0.

[3] D. Maclaurin, D. Duvenaud, and R. P. Adams. Gradient-based hyperparameter optimization through reversible learning. *Proceedings of the 32nd International Conference on Machine Learning*, PMLR 37, 2113–2122, 2015. https://proceedings.mlr.press/v37/maclaurin15.html.

[4] A. R. Calderbank, I. Daubechies, W. Sweldens, and B.-L. Yeo. Wavelet transforms that map integers to integers. *Applied and Computational Harmonic Analysis* 5, 332–369, 1998. doi:10.1006/acha.1997.0238. Author preprint: https://cm-bell-labs.github.io/who/wim/papers/integer.pdf.

[5] P. Mayekar, A. T. Suresh, and H. Tyagi. Wyner-Ziv estimators: efficient distributed mean estimation with side-information. *Proceedings of the 24th International Conference on Artificial Intelligence and Statistics*, PMLR 130, 3502–3510, 2021. https://proceedings.mlr.press/v130/mayekar21a.html.

[6] O. Ordentlich and U. Erez. Integer-forcing source coding. arXiv:1308.6552, 2013. https://arxiv.org/abs/1308.6552.

[7] R. Zamir, S. Shamai, and U. Erez. Nested linear/lattice codes for structured multiterminal binning. *IEEE Transactions on Information Theory* 48(6), 1250–1276, 2002. doi:10.1109/TIT.2002.1003821.

[8] B. Bollobás and A. Thomason. Projections of bodies and hereditary properties of hypergraphs. *Bulletin of the London Mathematical Society* 27(5), 417–424, 1995. doi:10.1112/blms/27.5.417.

[9] S. Brazitikos, A. Giannopoulos, and D.-M. Liakopoulos. Uniform cover inequalities for the volume of coordinate sections and projections of convex bodies. arXiv:1606.03779, 2016. Theorem 1.1, equation (1.5). https://arxiv.org/abs/1606.03779.

[10] E. Gover and N. Krikorian. Determinants and the volumes of parallelotopes and zonotopes. *Linear Algebra and its Applications* 433(1), 28–40, 2010. doi:10.1016/j.laa.2010.01.031.

[11] T. Bray, editor. The JavaScript Object Notation (JSON) data interchange format. RFC 8259, December 2017. https://www.rfc-editor.org/rfc/rfc8259.html.